



# Applicability of double layer capacitance measurements to monitor local temperature changes at polymer electrolyte membrane fuel cell cathodes

Jarek P. Sabawa<sup>a,\*</sup>, Aliaksandr S. Bandarenka<sup>a,b,\*</sup>

<sup>a</sup> Physics of Energy Conversion and Storage, Physik-Department, Technische Universität München, James-Franck-Str. 1, 85748 Garching, Germany

<sup>b</sup> Catalysis Research Center TUM, Ernst-Otto-Fischer-Straße 1, 85748 Garching, Germany



## ARTICLE INFO

### Keywords:

PEM fuel cells  
Electrical double layer capacitance  
Electrochemical impedance spectroscopy  
PEMFC temperature determination

## ABSTRACT

One of the most sensitive parameters to control the performance of automotive-size polymer electrolyte membrane fuel cells (PEMFCs) is the cell temperature. For instance, when starting up the fuel cell, it is critical to know whether the cell temperature is below ~273 K or, approaches the operating conditions. The easiest way to determine this is to perform measurements using some commercially available temperature sensors at the active electrode surface. However, this only applies to single-cells and not for automotive fuel cell stacks with ~400 cells. In this case, the measurement with a standard resistive temperature sensor is practically problematic. In this paper, we demonstrate that the electric double layer capacitance of the PEMFC cathodes (geometric active area size of 43.6 cm<sup>2</sup>) increases linearly from 268 K up to 333 K; and using this information, it is possible to determine the catalyst temperature accurately within this temperature range. These results should be of particular significance for both modelling the double layer in the PEMFCs as well as for the practical use in automotive applications.

## 1. Introduction

The cell temperature of a PEMFC is one of its most important operating parameters. Any related processes such as the hydrogen oxidation reaction (HOR), the transport of protons through the membrane or the oxygen reduction reaction (ORR) at the cathode side are strongly dependent on the reaction temperature. Therefore, the temperature measurements after shut-down and longer standing time on each automotive cell of a fuel cell stack at outside temperatures below or close to 273 K can be of immense importance. The inner cells could still be well above 273 K, whereby the outer cells could already be below this value. To prevent cathode degradation at low temperatures, it would be useful to know the cell temperature before the start-up [1–3]. The simplest way to measure the temperature of the cells would be to use a commercially available resistive temperature sensor placed near the active surface area. However, in an automotive full-scale stack (active surface area of ~300 cm<sup>2</sup>) with ~400 cells, where the space is limited, the measurement of each cell temperature with a standard temperature sensor is very difficult. The other possibility is the measurement of the stack coolant temperature. However, the measured

coolant temperature does not correspond to the actual temperature of the membrane or catalyst layers. The cell impedance measurements offer an attractive way of determining the cell temperature without the use of the temperature sensors. The double layer capacitance ( $C_{dl}$ ), which can be estimated from the impedance data, demonstrates a pronounced temperature dependence; and it can also be used when there is no oxygen present at the cathode, since the contribution of the Pt-catalyst to this measurement can be considered as minor [4–6]. This makes  $C_{dl}$  especially suitable for determining of the temperature and, therefore, of particular significance for the practical use in automotive applications. In this work, the relationship between the  $C_{dl}$  and the cell temperature is shown, as well as the ability to determine the cell temperature after shut-down using electrochemical impedance spectroscopy (EIS). For the analysis of the measured impedance data, a physical impedance model consisting of 5 equivalent circuit elements was used. Surprisingly, the electric double layer capacitance of the PEMFC cathodes increases linearly (and reversibly) from 268 K up to 333 K; and using this finding it is possible to accurately determine the cell temperature of PEMFC single-cells and stacks of different sizes without commercial resistive temperature sensors.

\* Corresponding authors at: Physics of Energy Conversion and Storage, Physik-Department, Technische Universität München, James-Franck-Str. 1, 85748 Garching, Germany (A.S. Bandarenka).

E-mail addresses: [ga53bux@mytum.de](mailto:ga53bux@mytum.de) (J.P. Sabawa), [bandarenka@ph.tum.de](mailto:bandarenka@ph.tum.de) (A.S. Bandarenka).

<https://doi.org/10.1016/j.rechem.2020.100078>

Received 30 July 2020; Accepted 29 October 2020

## 2. Experimental

A FuelCon Evaluator C1000-LT with an EIS capable load and the Peltier-Element-Tempered (PET) PEM single-cell was used [7]. With PET PEM single-cell, it was possible to achieve the exact temperature steps between 268 K and 333 K with an accuracy of  $\pm 0.2$  K. To ensure an even distribution of the gases, a low-pressure drop 14-channel flow field integrated in the anode and cathode monopolar plate was used. A membrane electrode assembly (MEA) with an active area size of 43.6 cm<sup>2</sup> with a  $\sim 15$   $\mu$ m thick polymer electrolyte membrane (anode/cathode platinum loading of 0.05/0.45 mg Pt/cm<sup>2</sup>) was utilized. On both sides of the coated catalyst membrane, there is a gas diffusion layer (GDL) with a microporous layer (MPL), with a total thickness of 235  $\mu$ m. The measurement was carried out fully automatically, controlled by the test bench software protocol (Fig. 1).

For each temperature step, the procedure loop was repeated three times (Fig. 1). The procedure, more exactly one temperature measurement cycle, can be divided into the parts described below.

### 2.1. Start-up & stable operation point (SOP)

The main function of the start-up procedure is to bring the cell to the standard working parameters in a defined reproducible manner (Fig. 1). The start-up was programmed in the way that it was not relevant if the cell was at a temperature way below 273 K or at 333 K. In the first phase, the cell was bypassed from the environmental conditions and heated up to a target temperature of 333 K. With the cell in bypass, the reactant gases were heated to the desired temperatures of 353 K. When the temperature of 333 K of the gas was exceeded, the anodes/cathodes humidification was switched on and set to dew point temperatures of 319 K (50% RH). On reaching the desired temperatures, the bypasses were opened and humidified H<sub>2</sub> and air were passed directly into the cell with the flow rates of  $\sim 8.3$  cm<sup>3</sup>/s and  $\sim 16.7$  cm<sup>3</sup>/s. When an open circuit voltage (OCV) of  $\sim 0.9$  V had been achieved, the outlet cell pressure was set with a defined ramp to 200 kPa and the current was ramped with a ramp rate of 0.0023 A/cm<sup>2</sup> per s to the current density of 0.5 A/cm<sup>2</sup> and then held for 3600 s. After this waiting time, the stable operation point (SOP) was executed and the load was switched to the aim current density of 0.8 A/cm<sup>2</sup>. This phase is particularly important to normalize the conditions in the cell and is, therefore, held for 4600 s.

### 2.2. Pre-conditioning procedure

Because of the sensitivity of the electrochemical impedance spectroscopy measurements to the cell water content and other working parameters, the pre-conditioning procedure is one of the most important steps in determining the temperature. Before the start of the pre-conditioning procedure, the load was set to 0 A (at OCV). After a stable OCV had been reached, the anode and cathode humidification was switched off and the outlet pressure as well as all heating systems were set to ambient conditions. To ensure low water content in the pipes, the cell was bypassed for a short time, and the pipes were purged with maximum H<sub>2</sub> and air flows to remove liquid water. After this, H<sub>2</sub> and air were passed back through the cell with a flow rate of 0.5 cm<sup>3</sup>/s and 28.7 cm<sup>3</sup>/s. This steps ensures that the humidity remains constant at the anode side, and the membrane water content is only controlled via the cathode air flow. During drying, the water content in the membrane is determined with the help of the measured impedance at frequency of 2 kHz. After reaching the desired high-frequency-resistance (HFR) of 150 mOhm, the cell was bypassed and equilibrated at the required temperature.

### 2.3. Determination of the cell impedance (DCI)

To stabilize the whole system, the cell was hold bypassed for 3600 s at the required temperature. After this waiting time, the bypasses from the anode and cathode were opened and reactants were directed into the cell. To ensure that the cell reached the OCV after opening the bypass valves, a waiting time of 60 s was selected before the measurement was started. The measurement of the impedance spectra was carried out within a frequency range between 10 kHz and 0.11 Hz at OCV with dry H<sub>2</sub> and air flows of 0.5 cm<sup>3</sup>/s and 2 cm<sup>3</sup>/s. A current amplitude of 20 mA was chosen for the entire impedance spectrum. The pressure as well the gas temperature were set to ambient operation parameters. With the ambient gas temperature, dehydration of the membrane and the protonic network in the catalyst layer could be avoided.

## 3. Results and discussion

With the measured impedance data at different temperatures and the physical equivalent circuit used in this work (shown in Fig. 2 (a)), the equivalent circuit parameters can be estimated [8,9]. The

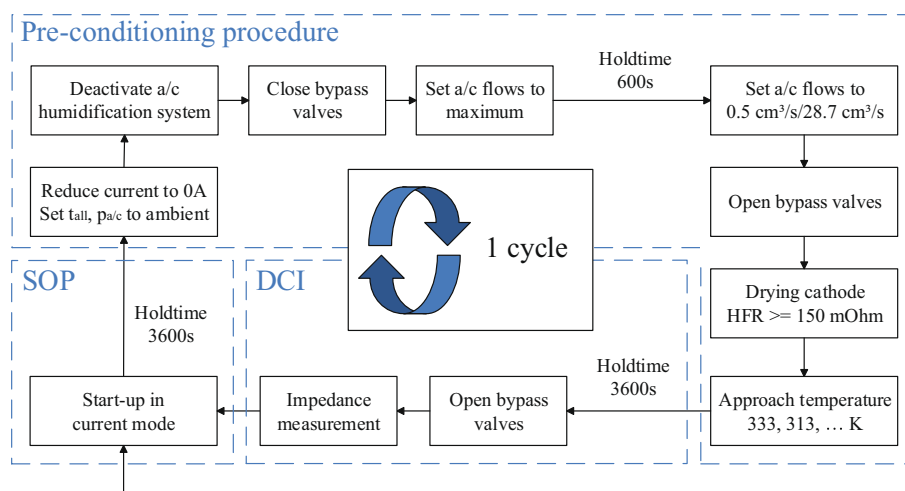
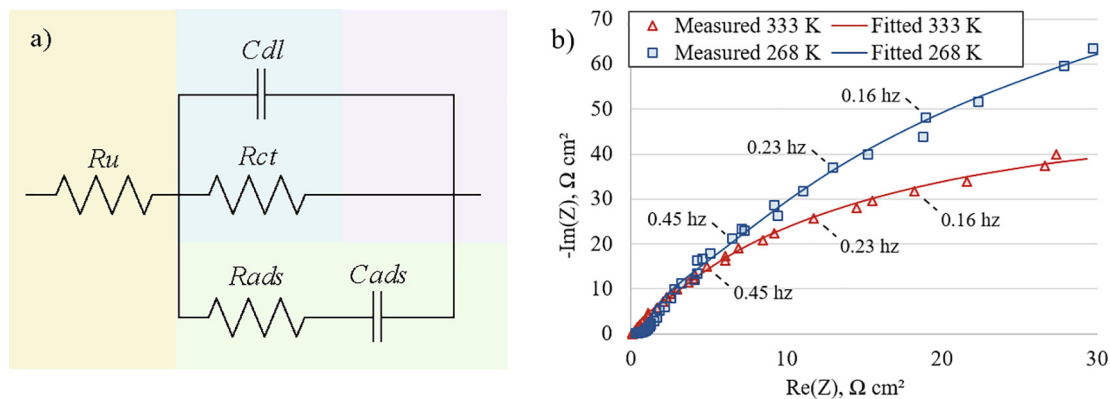


Fig. 1. Simplified description of the procedure loop (start-up followed by the stable operation point to normalize the conditions in the cell, pre-conditioning to keep identical measurement parameters, impedance measurements at the desired temperature and at the open circuit voltage).



**Fig. 2.** (a) Physical impedance model consisting of 5 equivalent circuit elements to fit the impedance data measured with the PEM single-cell at OCV:  $R_u$  – uncompensated (electrolyte) resistance,  $C_{dl}$  – electrical double layer capacitance,  $R_{ct}$  – the charge transfer resistance due to the oxygen reduction reaction at the cathode side,  $R_{ads}$  and  $C_{ads}$  are the adsorption resistance and capacitance, respectively, describing the impedance response due to possible specific quasi-reversible adsorption of the sulfonate-groups of Nafion at the Pt-electrocatalyst surface [12]. (b) Typical examples of the impedance spectra (open symbols) together with the fitting to the equivalent circuit (solid lines).

model shown in the figure has been reported recently [7,10]. The elements of the model are defined as follows:  $R_u$  is the uncompensated (electrolyte) resistance,  $C_{dl}$  – the double layer capacitance, and the Faradaic contribution  $R_{ct}$  is the charge transfer resistance due to the oxygen reduction reaction (ORR) and  $R_{ads}$  and  $C_{ads}$  are the elements accounting for the possible specific quasi-reversible adsorption of the sulfonate-groups of Nafion at the Pt-electrocatalyst surface, which has a relatively small but not negligible influence on the impedance response. The identification of the elements was done with EIS Data Analysis 1.3 software [11]. Fig. 2(b) shows examples of the fitting of the impedance data to the model. It shows that the spectra taken at the OCV differ considerably when the cell temperature is changed and can be fitted very well with the used model.

It emerges that both, the visible quality of the spectra shown in Fig. 2(b) as well as the error values of the fit calculated by the software are sufficiently low for every fitted spectrum. One requirement for the accuracy and good reproducibility of the low-frequency points is the consistent pre-conditioning procedure and the stable operation parameters during the impedance measurements [13].

The temperature dependencies of the equivalent circuit parameters (with the exception of the double layer capacitance  $C_{dl}$ , which will be discussed later) are shown in Fig. 3.

The uncompensated resistance  $R_u$  (mainly related to the Nafion® electrolyte) shows a significant decrease with the cell temperature (see Fig. 3(a)), as expected for the proton conductivity under humidification. One interpretation of this phenomenon discussed in the literature is that when the membrane is cold, the repulsive energy between the hydrophobic- and hydrophilic-parts of the matrix domains exists, and a lesser amount of water can be absorbed at the hydrophilic sulfonate-groups. At higher temperatures, more hydrophilic groups disperse into the hydrophobic matrix (entropically driven). This leads to an increase in the amount of absorbed water molecules at the hydrophilic groups; thereby the proton conductivity increases [14–16]. However, the determination of the exact individual high-frequency resistances such as the membrane resistance and the exact protonic pathway resistance in the catalyst layer isn't possible with the used impedance model in this work. A change of the R-C-elements, which are related to the specific quasi-reversible adsorption of the sulfonate-groups of Nafion at the Pt-electrocatalyst, can also be observed with different temperatures (see Fig. 3(c), (d)) [12]. Since the  $R_{ads}$  and  $C_{ads}$  are sensitive to the rest humidity in the system, the interpretation of the dependencies for both parameters are rather difficult in this work. In contrast, the temperature dependence of the charge transfer resistance  $R_{ct}$ , which is mainly related to the oxygen

reduction reaction and shown in Fig. 3(b), is rather expectable. The charge transfer resistance at a defined electrode potential ( $E$ ) can be given as follows [17]:

$$R_{ct}(E) = \frac{RT}{n^2 F^2 \alpha k(E, T) C_s(E, T) A_{sc}(E)} \quad (1)$$

with the transfer coefficient,  $\alpha$ , the active surface area of the Pt catalyst,  $A_{sc}$ , the surface concentration of oxygen,  $C_s$ , the number of electrons,  $n$ , the Faraday constant,  $F$ , and the rate coefficient,  $k$ , which temperature dependence can be described by the Arrhenius equation [18]. All parameters in Eq. (1) with the exception of the temperature,  $T$ , the concentration of oxygen,  $C_s$ , which should have a small influence at OCV, and the rate coefficient,  $k$ , should behave consistently at the measured temperature points. Due to the quantitative relationship between the local catalyst temperature and the activation energy, the rate coefficient  $k$  changes significantly with temperature, leading to a corresponding change in  $R_{ct}$ . However, if one would aim to use  $R_{ct}$  as an indicator for the temperature in the automotive applications, the temperature determination would only work if the constant amount of oxygen is available as the reactant. On the other hand, the  $R_{ct}$  is much more sensitive to the degradation of the catalyst layer compared to the  $C_{dl}$ . More exactly: The  $C_{dl}$  is formed between the carbon and ionomer interface. Due the reduction of electrochemical active surface area (ECSA) during the testing (e.g. Ostwald ripening), the  $R_{ct}$  will change at the OCV, whereby the  $C_{dl}$  should remain constant [19]. For this purpose, it makes sense to consider the  $C_{dl}$  as an indicator for the temperature measurements.

It is now interesting to analyze the measured temperature dependence of the double layer capacitance ( $C_{dl}$ ) shown in Fig. 4. The temperature dependence of the  $C_{dl}$  is more simple and quasi-linear, in contrast to those calculated using various approximations (e.g. mean spherical approximation (MSA)) and, moreover, it is rather reversible in the heating-cooling cycles [20].

We suppose, that the observed experimental dependence in the case of the  $C_{dl}$  of the PEMFC cathodes is the consequence of several influencing factors. In that context, two main mechanisms could be responsible for the behavior of the measured  $C_{dl}$ : Firstly, the fraction of free ions strongly decreases at low temperatures, which leads to a capacity decrease. Secondly, the impact of the volume change triggered by the different temperatures cannot be neglected. This means that due to the volume reduction towards lower temperatures, a smaller amount of sulfonate-groups comes into the contact with the electrically conductive carbon surface, which leads to a reduction in interface and thus the capacity. While the empirical finding of this work can be

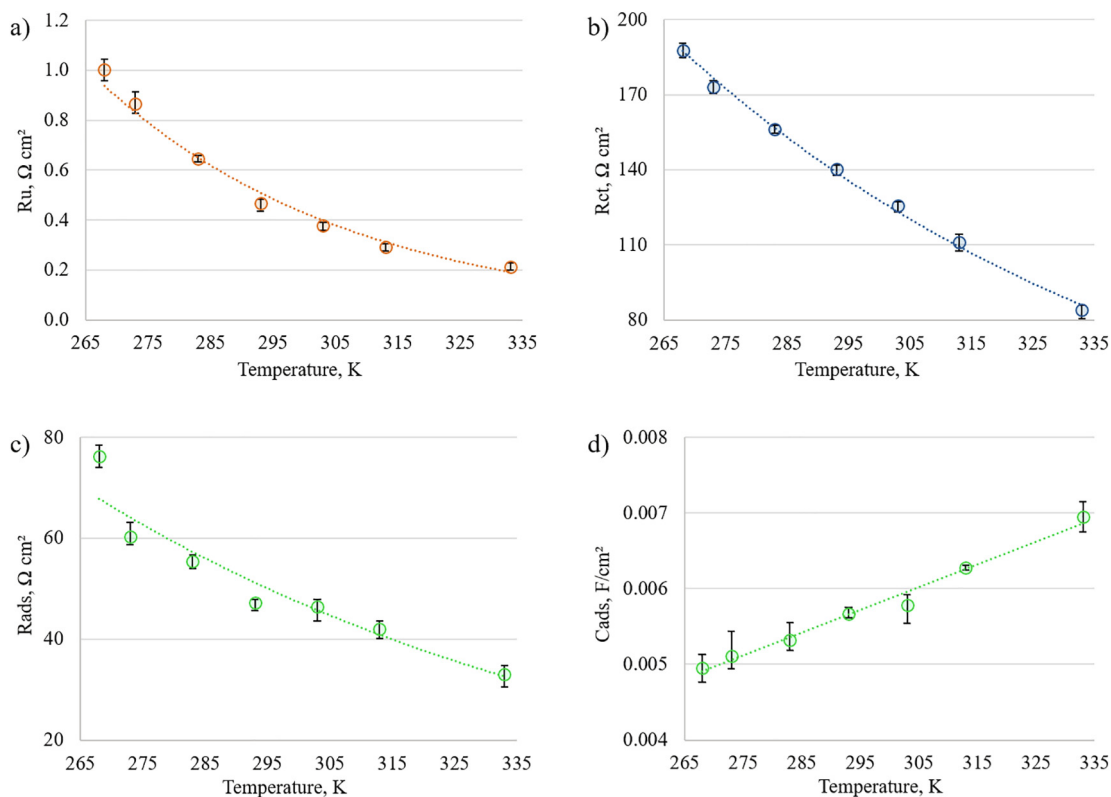


**Fig. 3.** The temperature dependences of the equivalent circuit parameters (in correspondence with Fig. 2 (a), excluding the double layer capacitance  $C_{dl}$ ). The dotted lines are given as the guides to eye.

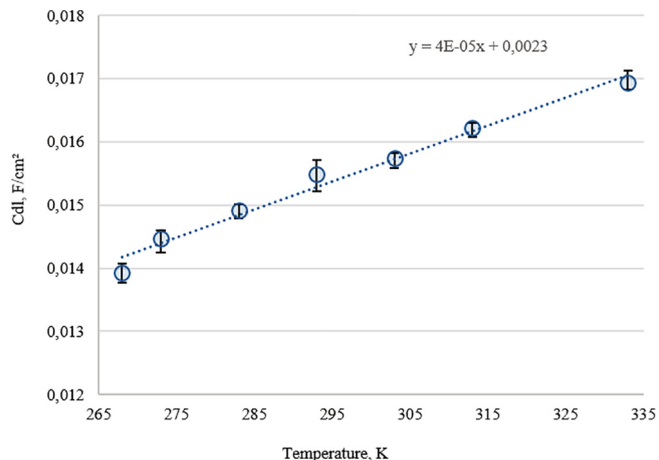


**Fig. 4.** Typical temperature dependence of the double layer capacitance  $C_{dl}$  in a temperature range from 265 up to 335 K of the PEMFC cathodes used in this work.

used to test PEMFCs under operating conditions, the fundamental understanding of the origin of this behavior requires further work. Thus, the dependence shown in Fig. 4 can be used as the calibration data for the accurate and relatively quick assessment of the PEMFC cathode temperature under operational conditions.

#### 4. Conclusions

A new method for determining the PEMFC cathode temperature after shutdown has been developed. With this method, impedance spectra at different temperatures are recorded and evaluated with a

relatively simple physical impedance model consisting of 5 equivalent circuit elements. In contrast to various approximations (e.g. mean spherical approximation (MSA)), a quasi-linear dependence of the double layer capacitance  $C_{dl}$  on the temperature was observed for the PEMFC cathodes. It has been also found that all other EC-elements are sensitive to the temperature changes. Based on this finding, a method for estimating the temperatures at the cathodes in the temperature range from 268 K to 333 K is proposed. It is based on the determination of the cell temperature using the double layer capacitance values.

#### Declaration of Competing Interest

The authors declare that they have no known competing financial interests or personal relationships that could have appeared to influence the work reported in this paper.

#### Acknowledgments

This work was funded by the German Research Foundation (DFG) and the Technische Universität München (TUM) within the Open Access Publication Program.

#### References

- [1] W. Schmittinger, A. Vahidi, A review of the main parameters influencing long term performance and durability of PEM fuel cells, *J. Power Sources* 180 (2008) 1–14.
- [2] Z. Wan, H. Chang, S. Shu, Y. Wang, H. Tang, A review on cold start of proton exchange membrane fuel cells, *Energies* 7 (2014) 3179–3203.
- [3] Q. Yan, H. Toghiani, Y. Lee, K. Liang, H. Causey, Effect of sub-freezing temperatures on a PEM fuel cell performance, startup and fuel cell components, *J. Power Sources* 160 (160) (2006) 1242–1250.
- [4] D. di Caprio, J. Stafiej, Z. Borkowska, Anomalous temperature dependence of differential capacity at an uncharged interface with Debye-Hückel electrolyte: field theoretical approach, *J. Electroanal. Chem.* 582 (2005) 41–49.

- [5] M. Chen, Z.A.H. Goodwin, G. Feng, A.A. Kornyshev, On the temperature dependence of the double layer capacitance of ionic liquids, *J. Electroanal. Chem.* 819 (2018) 347–358.
- [6] J. Reszko-Zygmunt, S. Sokolowski, D. Henderson, D. Boda, Temperature dependence of the double layer capacitance for the restricted primitive model of an electrolyte solution from a density functional approach, *J. Chem. Phys.* 8 (2005) 122.
- [7] J.P. Sabawa, A.S. Bandarenka, Degradation mechanisms in polymer electrolyte membrane fuel cells caused by freeze-cycles: Investigation using electrochemical impedance spectroscopy, *Electrochim. Acta* 311 (2019) 21–29.
- [8] A. Lasia, *Electrochemical Impedance Spectroscopy and its Applications*, Springer, 2014, p. 367.
- [9] A.A. Moya, Electrochemical impedance of ion-exchange membranes with interfacial charge transfer resistances, *J. Phys. Chem. C* 120 (2016) 6543–6552.
- [10] M. Obermaier, A.S. Bandarenka, C. Lohri-Tymozhynsky, A comprehensive physical impedance model of polymer electrolyte fuel cell cathodes in oxygen-free atmosphere, *Sci. Rep.* 8 (2018) 4933.
- [11] A.S. Bandarenka, Development of hybrid algorithms for EIS data fitting, a book chapter, in: O. Kanoun (Ed.), *Lecture Notes on Impedance Spectroscopy. Measurement, Modeling and Applications*, CRC Press, Taylor and Francis Group, London, 2013, pp. 29–36.
- [12] J. Tymoczko, F. Calle-Vallejo, V. Colic, M.T.M. Koper, W. Schuhmann, A.S. Bandarenka, Oxygen reduction at a Cu modified Pt(111) model electrocatalyst in contact with NAFION polymer, *ACS Catal.* 4 (2014) 3772–3778.
- [13] D. Aaron, S. Yiacoumi, C. Tsouris, Effects of proton-exchange membrane fuel cell operating conditions on charge transfer resistance measured by electrochemical impedance spectroscopy, *Sep. Sci. Technol.* 43 (2008) 9–10.
- [14] T.D. Gierke, G.E. Munn, F.C. Wilson, The morphology in Nafion perfluorinated membrane products, as determined by wide- and small-angle x-ray studies, *J. Polym. Sci.* 19 (1981) 1687–1704.
- [15] W.Y. Hsu, T.D. Gierke, Ion transport and clustering in Nafion perfluorinated membranes, *J. Membr. Sci.* 13 (1983) 307–326.
- [16] S. Cui, J. Liu, M.E. Selvan, D.J. Keffer, B.J. Edwards, W.V. Steele, A molecular dynamics study of nafion polyelectrolyte membrane and the aqueous phase structure for proton transport, *J. Phys. Chem. B* 111 (2007) 2208–2218.
- [17] D. Vladikova, The technique of the differential impedance analysis Part I: Basics of the impedance spectroscopy, in: *Proceedings of the International Workshop on Advanced Techniques for Energy Sources Investigation and Testing*, 2004, pp. 1–28.
- [18] K.J. Laidler, The development of the Arrhenius equation, *J. Chem. Educ.* 61 (1984) 494.
- [19] B.B. Berkes, J.B. Hery, M. Huang, A.S. Bondarenko, Electrochemical characterisation of copper thin-film formation on polycrystalline platinum, *ChemPhysChem* 13 (2012) 3210–3217.
- [20] M. Holovko, V. Kapko, D. Henderson, D. Boda, On the influence of ionic association on the capacitance of an electrical double layer, *Chem. Phys. Lett.* 341 (2001) 363–368.